# Leveraging Distribution Alignment via Stein Path for Cross-Domain Cold-Start Recommendation

**Weiming Liu, Jiajie Su, Chaochao Chen, and Xiaolin Zheng***
Zhejiang University, Hangzhou, China
{21831010,sujiajie,zjuccc,xlzheng}@zju.edu.cn

## Abstract

Cross-Domain Recommendation (CDR) has been popularly studied to utilize different domain knowledge to solve the cold-start problem in recommender systems. In this paper, we focus on the *Cross-Domain Cold-Start Recommendation* (*CDCSR*) problem. That is, how to leverage the information from a source domain, where items are 'warm', to improve the recommendation performance of a target domain, where items are 'cold'. Unfortunately, previous approaches on cold-start and CDR cannot reduce the latent embedding discrepancy across domains efficiently and lead to model degradation. To address this issue, we propose `DisAlign`, a cross-domain recommendation framework for the CDCSR problem, which utilizes both rating and auxiliary representations from the source domain to improve the recommendation performance of the target domain. Specifically, we first propose Stein path alignment for aligning the latent embedding distributions across domains, and then further propose its improved version, i.e., proxy Stein path, which can reduce the operation consumption and improve efficiency. Our empirical study on Douban and Amazon datasets demonstrates that `DisAlign` significantly outperforms the state-of-the-art models under the CDCSR setting.

## 1 Introduction

Data sparsity and cold-start are long-standing problems in recommender systems [15, 19]. With the development of internet techniques, most users always participant in many platforms or domains for different purposes. Therefore, Cross-Domain Recommendation (CDR) has emerged to utilise the relatively richer information from a source domain to improve the recommendation accuracy in a target domain [52, 53]. Most existing CDR models can tackle the data sparsity problem in the target domain by assuming the existence of overlapped users or items with similar tastes or attributions across domains [5].

Instead of focusing on solving the data sparsity problem, we consider cold-start item recommendation under the CDR setting. Specifically, we concentrate on the *Cross-Domain Cold-Start Recommendation* (*CDCSR*) problem, that is, two domains share the same user set but different items, and both domains have auxiliary representations such as item profiles or descriptions. The prime challenge is how to leverage the information from the source domain, where the items are 'warm', to improve the recommendation performance of the target domain, where the items are 'cold'. The CDCSR problem popularly exists in practice, for instance, a movie marketing platform newly launches a book renting service where there is no user-book interaction yet, as shown in Figure 1.

Existing researches on cold-start recommendation and CDR cannot solve the above problem well. On the one hand, existing cold-start recommendation models assume that the distributions of cold items should be consistent with the warm ones as they are homogeneous [54, 18, 12]. On the other hand,

*Corresponding Author

35th Conference on Neural Information Processing Systems (NeurIPS 2021), Sydney, Australia.

existing CDR models assume that both source and target domains have user-item interactions for learning the mapping functions [25]. Since the cold and warm items are heterogeneous with different latent embedding distributions in practice, and there is no user-item interaction in the target domain, conventional cold-start and CDR models cannot properly suitable to the CDCSR problem.

Similar to the transfer learning task, the key to the CDCSR problem is to reduce the discrepancy between the latent embedding distributions across domains. However, both the warm and cold item representations are scattered and complicated due to the fact that the latent embeddings may represent diverse information. Thus, existing transfer learning based domain adaptation approaches [23, 45, 37] cannot achieve good alignment results, which limits their performances.

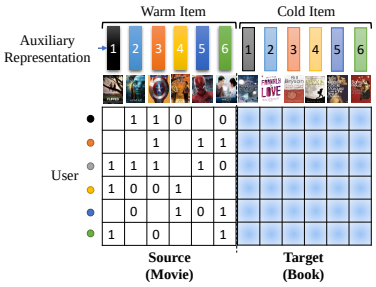

Figure 1: The CDCSR Problem.

To address the aforementioned issue, in this paper, we propose `DisAlign`, a cross-domain recommendation framework for the CDCSR problem. In order to better align the complicated latent embedding distributions and make high quality of rating predictions, we utilize two modules in `DisAlign`, i.e., *rating prediction module* and *embedding distribution alignment module*, as will be shown in Figure 2. The rating prediction module aims to capture user and item collaborative preferences in the source domain, and we propose metric-based contrastive learning for modelling. The goal of distribution alignment module is to properly match the latent embedding distributions across domains, and we propose two techniques for it, i.e., *Stein path alignment* and its improved version called *proxy Stein path alignment*. Specifically, inspired by the particle-based inference algorithm Stein Variational Gradient Descent (SVGD) [21, 13, 20], we first propose Stein path alignment to minimize the domain discrepancy through the particle-moving process, which can take both the source probability and target intra-domain structure into account. Although Stein path can obtain satisfying performance, it has to involve all the target samples during the training process, which is time consuming when data size is large. Thus, we further propose proxy Stein path alignment which only needs to exploit typical samples to represent the target data distribution, and thus can accelerate the operation speed. The comparison and visualization results in experiments will show the reliability and efficiency of `DisAlign`.

We summarize the main contributions of this paper as follows: (1) We propose a novel framework, i.e., `DisAlign`, for the CDCSR problem, which can utilize both rating and auxiliary representations from the source domain to improve the recommendation performance of the target domain. (2) To our best knowledge, this is the first attempt in literature to propose Stein path alignment for aligning the latent embedding distributions across domains, and we also propose its improved version, i.e., proxy Stein path, for higher efficiency. (3) Empirical studies on Douban and Amazon datasets demonstrate that `DisAlign` significantly improves the state-of-the-art models under the CDCSR setting.

## 2 The proposed model

### 2.1 Framework of DisAlign

First, we describe notations. We assume there are two domains, i.e., a source domain $\mathcal{S}$ and a target domain $\mathcal{T}$. We assume both domains $\mathcal{S}$ and $\mathcal{T}$ have $N_U$ users, $\mathcal{S}$ has $N_S$ warm items, and $\mathcal{T}$ has $N_T$ cold items. Let $\boldsymbol{R}^{\mathcal{S}} \in \mathbb{R}^{N_U \times N_S}$ be the warm rating matrix in $\mathcal{S}$ and $\boldsymbol{R}^{\mathcal{T}} \in \mathbb{R}^{N_U \times N_T}$ be the cold rating matrix in $\mathcal{T}$. In CDCSR setting, $\boldsymbol{R}^{\mathcal{T}}$ is absence during training and will be only used for test, since items are cold in $\mathcal{T}$. We also assume that the warm items and the cold items have auxiliary representations $\boldsymbol{X}^W \in \mathbb{R}^{N_S \times Z}$ and $\boldsymbol{X}^V \in \mathbb{R}^{N_T \times Z}$, respectively, with $Z$ denoting the dimension of auxiliary representations. The auxiliary representations usually include useful side-information, e.g., themes, reviews, profiles in a movie domain. Our purpose is to predict the absent $\boldsymbol{R}^{\mathcal{T}}$ in $\mathcal{T}$ by leveraging $\boldsymbol{R}^{\mathcal{S}}$ in $\mathcal{S}$ and the auxiliary representations in both $\mathcal{S}$ and $\mathcal{T}$.

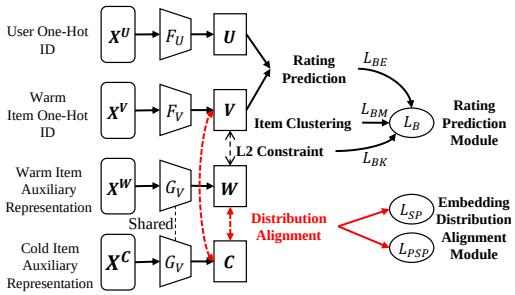

Figure 2: The Framework of `DisAlign`.

Then, we introduce the overview of our proposed DisAlign framework, as is illustrated in Figure 2. DisAlign model mainly has two modules, i.e., *rating prediction module* and *embedding distribution alignment module*. To avoid the error superimposition problem [54], the rating prediction module in the source domain mainly provides end-to-end joint training of modelling user and item collaborative embeddings and matching the item collaborative embeddings with item auxiliary embeddings. The embedding distribution alignment module aligns the distributions between the warm and cold items across domains, minimizing the discrepancy between auxiliary latent feature embeddings in the source and target domains sufficiently. We will introduce these two modules in details later.

### 2.2 Rating prediction module

We first introduce the rating prediction module of DisAlign. For the $i$-th user and the $j$-th item in the source (warm) domain, we define their corresponding one-hot ID vectors as $\boldsymbol{X}_i^U$ and $\boldsymbol{X}_j^V$, respectively. For the $j$-th warm item, we also define its auxiliary representation as $\boldsymbol{X}_j^W$. The rating prediction module mainly has three purposes, including (1) exploiting user and item collaborative embeddings based on ratings, which is the prime purpose; (2) matching the item collaborative embeddings with item auxiliary embeddings; and (3) obtaining more discriminative item collaborative embeddings using unsupervised clustering method.

First, user and item collaborative embeddings should accurately represent the corresponding rating interactions. We obtain the user and item collaborative embeddings by $F_U(\boldsymbol{X}^U) = \boldsymbol{U} \in \mathbb{R}^{N\times D}$ and $F_V(\boldsymbol{X}^V) = \boldsymbol{V} \in \mathbb{R}^{N\times D}$, respectively. Here, $F_U$ and $F_V$ denote the user and item encoding networks respectively, $N$ is batch size, and $D$ is the dimension of collaborative embeddings. After that, we use pairwise ranking loss $L_{BE}$ based on metric-based contrastive learning [10, 14]:

$$\min L_{BE} = -\sum_{(\boldsymbol{U}_i,\boldsymbol{V}_j,\boldsymbol{V}_k)\in\mathcal{D}} \log \frac{\exp\langle \boldsymbol{U}_i, \boldsymbol{V}_j\rangle}{\exp\langle \boldsymbol{U}_i, \boldsymbol{V}_j\rangle + \exp\langle \boldsymbol{U}_i, \boldsymbol{V}_k\rangle}, \tag{1}$$

where $\mathcal{D} := \{(\boldsymbol{U}_i, \boldsymbol{V}_j, \boldsymbol{V}_k) | R_{ij}^{\mathcal{S}} > R_{ik}^{\mathcal{S}}\}$ denotes the original preference pairs [32], and $\langle\cdot,\cdot\rangle$ denotes the inner product. The loss function $L_{BE}$ can pull the positive items close and push the negative items away for a certain user according to his/her preference.

Second, a item's collaborative embedding should be similar to its auxiliary embeddings to avoid the error superimposition problem [54]. We utilize a network $G_V$ to translate the auxiliary representations into auxiliary embeddings as $G_V(\boldsymbol{X}^W) = \boldsymbol{W} \in \mathbb{R}^{N\times D}$. After it, the item embedding matching loss is given by $L_{BM} = ||\boldsymbol{W} - \boldsymbol{V}||_2^2$.

Third, similar item collaborative embeddings should be clustered in order to obtain more discriminative latent features. We adopt deep unsupervised K-Means clustering approach [24, 48] for this, and the corresponding loss is $\min_{\boldsymbol{F}\boldsymbol{F}^T=\boldsymbol{I}} L_{BK} = \left[\mathrm{Tr}(\boldsymbol{V}\boldsymbol{V}^T) - \mathrm{Tr}(\boldsymbol{F}\boldsymbol{V}\boldsymbol{V}^T\boldsymbol{F}^T)\right]$, where $\boldsymbol{F} \in \mathbb{R}^{K\times N}$ is the cluster indicator matrix and $K$ denotes the cluster number.

In summary, the loss of the rating prediction module is a combination of the three losses, that is:

$$\min_{\boldsymbol{F}\boldsymbol{F}^T=\boldsymbol{I}} L_B = L_{BE} + \eta L_{BM} + \zeta L_{BK}, \tag{2}$$

where $\zeta$ and $\eta$ represent the balance hyper-parameters. The optimization procedure is given as below: (1) Fixing the other variables except $\boldsymbol{F}$, we update $\boldsymbol{F}$ through $\min_{\boldsymbol{F}\boldsymbol{F}^T=\boldsymbol{I}} \mathrm{Tr}(\boldsymbol{F}\boldsymbol{V}\boldsymbol{V}^T\boldsymbol{F}^T)$ with singular value decomposition algorithm; (2) Fixing $\boldsymbol{F}$, we update other variables through gradient descent methods for several iterations then go back to step (1) until it convergences. For the sake of stability, in practice, we update $\boldsymbol{F}$ every 15 iterations.

### 2.3 Embedding distribution alignment module

#### 2.3.1 Overview

We then introduce the embedding distribution alignment module of DisAlign. We use $G_V(\boldsymbol{X}_j^C) = \boldsymbol{C} \in \mathbb{R}^{N\times D}$ to denote the auxiliary embeddings of the cold items in the target domain. Specifically, $G_V(\cdot)$ is a two-stream siamese network with shared weights for encoding both warm item auxiliary representation $\boldsymbol{X}^W$ and cold item auxiliary representation $\boldsymbol{X}^C$. We denote $p_W$ and $p_C$ as the warm and cold item auxiliary embedding probability distributions, respectively, and denote $p_V$ as the warm

item collaborative embedding probability distribution. In CDCSR setting, $p_W \neq p_C$ and $p_V \neq p_C$, because the embeddings generated from the source (warm) domain and the target (cold) domain are heterogeneous, which leads to the *domain discrepancy* problem. Let us consider a case where the source domain has user-book interactions while the target domain has user-movie interactions. Although books and movies share some similar characteristics, the auxiliary representations of the Book domain usually include authors and writing styles, while the auxiliary representations of the Movie domain include directors and actors, which brings discrepancy. Without embedding distribution alignment, a recommender system may recommend horror books instead of history books to a user who likes history movies rather than horror movies due to domain discrepancy, as illustrated in the left of Figure 3. After alignment, the history movies/books and horror movies/books are aligned, as is shown in the right of Figure 3, and thus the recommender system can provide more reliable results. In order to reduce the distribution discrepancy between the source and target domains, we introduce two approaches, i.e., Stein path alignment and Proxy stein path alignment.

### 2.3.2 Stein path alignment

As mentioned in Section 1, since the latent embeddings from two domains in CDCSR are scattered and complicated due to the fact that they may represent diverse information, previous domain adaptation methods cannot be effectively utilized to solve the distribution discrepancy problem. Therefore, we propose a new distribution alignment approach, named *Stein path alignment*. Stein path alignment can prompt the target samples move to the source domain through proper *paths*, according to the target intra-domain structure and the probability distribution of the source domain. Stein path alignment relies on Stein Variational Gradient Descent (SVGD) [21, 42], a variational inference method that starts from a set of initial particles and iteratively updates them with an approximate steepest direction, whose main iteration process is:

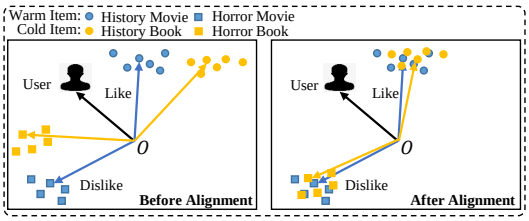

Figure 3: Demonstration of the necessity of embedding distribution alignment.

$$\boldsymbol{z}_{i,l} = \boldsymbol{z}_{i,l-1} + \epsilon \phi_p(\boldsymbol{z}_{i,l-1}),\ \ \phi_p(\boldsymbol{z}) = \frac{1}{N}\sum_{j=1}^{N}\left[k(\boldsymbol{z},\boldsymbol{z}_j)\nabla_{\boldsymbol{z}}\log p(\boldsymbol{z}) + \nabla_{\boldsymbol{z}} k(\boldsymbol{z},\boldsymbol{z}_j)\right], \tag{3}$$

where $\boldsymbol{z}_{i,l}$ denotes the $i$-th original target sample at the $l$-th iteration, $p(\boldsymbol{z})$ denotes the source probability distribution, $\epsilon$ denotes the step size, and $k(\boldsymbol{x},\boldsymbol{y}) = \exp\left(-(||\boldsymbol{x}-\boldsymbol{y}||_2^2)/\sigma^2\right)$ is the Gaussian kernel function with $\sigma$ denoting the bandwidth. Existing researches [21, 7, 2] have proved that mean field theory can guarantee the rigorous theoretical convergence of SVGD, that is, the gradient dynamics at particle level will approach to zero: $\lim_{t\to+\infty}(1/N \times \sum_{i=0}^{N}\phi_p(\boldsymbol{z}_{i,t})) \to 0$.

**Stein path distance.** We denote $\boldsymbol{z}_{i,t}$ as the Stein mirror point of $\boldsymbol{z}_{i,0}$ when SVGD convergences at the $t$-th iteration. We propose *Stein path distance* as below:

$$\mathcal{P}_{\mathcal{T}\to\mathcal{S}}(\boldsymbol{Z}) := \frac{1}{N}\sum_{i=0}^{N}||\boldsymbol{z}_{i,t}-\boldsymbol{z}_{i,0}||_2^2 = \frac{1}{N}\sum_{i=0}^{N}||\boldsymbol{z}_{i,t-1}+\epsilon\phi_{\mathcal{S}}(\boldsymbol{z}_{i,t-1})-\boldsymbol{z}_{i,0}||_2^2\,. \tag{4}$$

Stein path distance quantifies the discrepancy between the source domain $\mathcal{S}$ and the target domain $\mathcal{T}$ by taking the average length of all paths from $\mathcal{T}$ to $\mathcal{S}$ through the $t$-th iteration. Stein path considers the source probability distribution and intra-domain structures, and thus can avoid negative transfer arisen from coarsely pairwise matching by traditional methods. Meanwhile Stein path is also explainable. Let $\boldsymbol{z}_{i,0}$ denote the auxiliary embedding of $i$-th book in the Book domain, $\boldsymbol{z}_{i,t}$ could be taken as a similar movie in the Movie domain, e.g., the movie is based on the story of the book. The calculation of Stein path distance mainly has three steps. First, adopting kernel density estimation [30, 29, 39] with radial basis function kernel to estimate the probabilities of $\boldsymbol{W}$ and $\boldsymbol{V}$. Second, finding the Stein mirror point of the cold item auxiliary embeddings through SVGD by Equation (3). Third, calculating the Stein path distance using Equation (4). The calculation details will be given in Appendix A.1.

**Stein path loss.** In summary, the better the source and target domains are aligned, the smaller the Stein path distance. Therefore, we innovatively propose *Stein path loss* to align the cold item auxiliary

embedding $\boldsymbol{C}$ with warm item collaborative preference $\boldsymbol{V}$ and auxiliary embedding $\boldsymbol{W}$ as below:

$$\min L_{SP} = \mathcal{P}_{C\to W}(\boldsymbol{C}) + \mathcal{P}_{C\to V}(\boldsymbol{C}) + ||\mathcal{P}_{C\to W}(\boldsymbol{C}) - \mathcal{P}_{C\to V}(\boldsymbol{C})||_2^2, \tag{5}$$

where the first two terms denote the Stein path distances from $\boldsymbol{C}$ to $\boldsymbol{W}$ and $\boldsymbol{C}$ to $\boldsymbol{V}$, respectively, and the third term reinforces that these two distances should be similar.

### 2.3.3 Proxy Stein path alignment

Although Stein path alignment achieves satisfying performance, it has scalability problem when facing large dataset. Because all the cold items in each batch need to be used for calculating Stein path distance. Therefore, it is urgent to reduce the computation cost to accelerate the optimization process. To do this, we propose *proxy Stein path approach* which only needs to choose the most typical cold item proxies to represent the global properties in order to speed up the alignment process through SVGD. We now describe the main steps for finding the proxies and the optimization procedure.

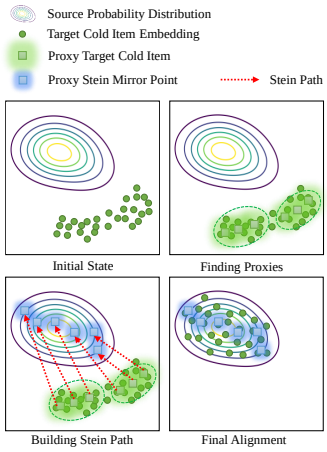


Figure 4: The main procedures of proxy Stein path alignment.

**Multiple-proxies algorithm.** We first introduce a highly efficient *multiple-proxies algorithm*, which aims to find typical proxy samples in the target domain. Suppose there exists $\boldsymbol{M} \in \mathbb{R}^{H\times D}$ typical proxies for the cold item auxiliary embeddings $\boldsymbol{C}$, where $H$ denotes the number of proxies. Let $\boldsymbol{\Psi} \in \mathbb{R}^{N\times H}$ be the similarity matrix between the cold items in the target domain and the proxies. Inspired by [1, 28], we formulate the multiple-proxies optimization problem as

$$\min_{\boldsymbol{M},\boldsymbol{\psi}_i^T\mathbf{1}=1,\psi_{ij}\geq 0} \sum_{i=1}^{N}\sum_{j=1}^{H}\psi_{ij}||\boldsymbol{c}_i - \boldsymbol{m}_j||_2^2 + \alpha\sum_{i=1}^{N}\sum_{j=1}^{H}\psi_{ij}\log\psi_{ij}, \tag{6}$$

where $\boldsymbol{c}_i$ denotes the $i$-th cold item auxiliary embedding and $\boldsymbol{m}_j$ denotes the $j$-th corresponding proxy. The entropy norm regularization term $\sum_{i=1}^{N}\sum_{j=1}^{H}\psi_{ij}\log\psi_{ij}$ is set to avoid trivial solution with $\alpha$ denoting the regularization strength. Compared with the square norm $||\cdot||_2$, the entropy norm can not only obtain a nonnegative and nonlinearly representational similarity matrix but also reduce the computational cost [1]. In summary, the multiple-proxies optimization algorithm has two main steps, i.e., (1) updating $\boldsymbol{\Psi}$, which has closed-form solution, and (2) updating $\boldsymbol{M}$ as $\boldsymbol{m}_j = \sum_{i=1}^{N}\psi_{ij}\boldsymbol{c}_i / \sum_{i=1}^{N}\psi_{ij}$. The optimization could be done by repeating (1) and (2) until $\boldsymbol{\Psi}$ and $\boldsymbol{M}$ convergence. We will present the optimization details in Appendix A.2.

**Proxy Stein path distance.** After finding the typical proxies $\boldsymbol{M}$ and setting $\boldsymbol{\Psi}$ as a constant, we propose *proxy Stein path distance* according to the original Stein path as below:

$$\mathcal{P}^*_{\mathcal{T}\to\mathcal{S}}(\boldsymbol{M}) = \frac{1}{H}\sum_{i=0}^{H}||\boldsymbol{m}_{i,t} - \boldsymbol{m}_{i,0}||_2^2 = \frac{1}{H}\sum_{i=0}^{H}||\boldsymbol{m}_{i,t-1} + \epsilon\phi_{\mathcal{S}}(\boldsymbol{m}_{i,t-1}) - \boldsymbol{m}_{i,0}||_2^2, \tag{7}$$

where $\boldsymbol{m}_{i,t}$ denotes the $i$-th proxy $\boldsymbol{m}_i$ at the $t$-th iteration. Notably, in each batch, proxy Stein path *only* needs to move the number of proxy samples ($H$) in the target domain rather than the total number of samples ($N$). Since $H < N$, proxy Stein path can reduce the time consumption on calculating the Stein path distance.

**Proxy Stein path loss.** Similarly to the Stein path loss, the *proxy Stein path loss* is given by:

$$\min L_{PSP} = \mathcal{P}^*_{C\to W}(\boldsymbol{M}) + \mathcal{P}^*_{C\to V}(\boldsymbol{M}) + ||\mathcal{P}^*_{C\to W}(\boldsymbol{M}) - \mathcal{P}^*_{C\to V}(\boldsymbol{M})||_2^2. \tag{8}$$

The optimization of proxy Stein path alignment mainly has four steps. The first step is adopting the multiple-proxies algorithm to figure out the typical proxies $\boldsymbol{M}$ in the target domain. The following three steps are similar as Stein path alignment mentioned in the Section 2.3.2, except that we are moving proxies $\boldsymbol{M}$ rather than $\boldsymbol{C}$. We will present the optimization details in Appendix A.3.

**Time complexity analysis.** The time complexity of Stein path alignment is $O(N^3 t_1)$, where $t_1$ is the iteration number. The time complexities of the multiple-proxies algorithm and proxy Stein path

Table 1: Experimental results on Douban and Amazon datasets.

| | (Douban) Movie→Book | | | (Douban) Movie→Music | | | (Douban) Book→Movie | | | (Amazon) Movie→Music | | |
|---|---|---|---|---|---|---|---|---|---|---|---|---|
| | HR | Recall | NDCG | HR | Recall | NDCG | HR | Recall | NDCG | HR | Recall | NDCG |
| DropoutNet | .2866 | .1528 | .0959 | .2893 | .1896 | .1134 | .2448 | .0976 | .0553 | .2591 | .1463 | .0786 |
| LLAE | .2914 | .1744 | .1078 | .3105 | .2039 | .1278 | .2511 | .1104 | .0618 | .2643 | .1504 | .0850 |
| Heater | .2983 | .1816 | .1135 | .3223 | .2104 | .1310 | .2613 | .1263 | .0707 | .2784 | .1631 | .0942 |
| WCF | .3028 | .1920 | .1266 | .3376 | .2177 | .1385 | .2704 | .1385 | .0796 | .2867 | .1744 | .1103 |
| ESAM | .3146 | .2025 | .1304 | .3467 | .2314 | .1491 | .2815 | .1482 | .0886 | .2942 | .1878 | .1186 |
| DARec | .3139 | .2149 | .1356 | .3350 | .2196 | .1389 | .2749 | .1407 | .0824 | .2981 | .1910 | .1229 |
| `DisAlign`-Base | .2991 | .1846 | .1189 | .3258 | .2108 | .1324 | .2617 | .1276 | .0733 | .2839 | .1676 | .1054 |
| `DisAlign`-SP(I) | .3375 | .2373 | .1466 | .3650 | .2485 | .1587 | .3023 | .1682 | .0979 | .3102 | .2096 | .1303 |
| `DisAlign`-SP | **.3428** | **.2411** | **.1508** | .3734 | .2506 | .1603 | .3028 | .1709 | .1058 | .3155 | .2182 | .1379 |
| `DisAlign`-PSP | .3401 | .2405 | .1482 | **.3795** | **.2528** | **.1623** | **.3102** | **.1711** | **.1076** | **.3281** | **.2276** | **.1395** |
| | (Douban) Book→Music | | | (Douban) Music→Movie | | | (Douban) Music→Book | | | (Amazon) Music→Movie | | |
| | HR | Recall | NDCG | HR | Recall | NDCG | HR | Recall | NDCG | HR | Recall | NDCG |
| DropoutNet | .2584 | .1215 | .0686 | .2595 | .1310 | .0767 | .2632 | .1196 | .0603 | .2662 | .1743 | .1005 |
| LLAE | .2685 | .1268 | .0710 | .2635 | .1424 | .0819 | .2717 | .1245 | .0658 | .2753 | .1802 | .1093 |
| Heater | .2724 | .1289 | .0742 | .2701 | .1472 | .0833 | .2834 | .1342 | .0733 | .2848 | .1876 | .1115 |
| WCF | .2710 | .1332 | .0761 | .2722 | .1530 | .0864 | .2726 | .1295 | .0728 | .2967 | .2112 | .1240 |
| ESAM | .2837 | .1398 | .0803 | .2876 | .1709 | .0935 | .2868 | .1486 | .0847 | .3273 | .2204 | .1415 |
| DARec | .2866 | .1410 | .0839 | .2918 | .1683 | .0916 | .2917 | .1409 | .0811 | .3313 | .2293 | .1476 |
| `DisAlign`-Base | .2712 | .1303 | .0745 | .2684 | .1490 | .0858 | .2746 | .1305 | .0697 | .2913 | .1928 | .1181 |
| `DisAlign`-SP(I) | .2946 | .1557 | .0881 | .3082 | .1932 | .1107 | .2986 | .1623 | .0957 | .3362 | .2414 | .1520 |
| `DisAlign`-SP | .2983 | .1581 | .0905 | .3107 | .1948 | .1156 | **.3073** | **.1692** | **.1015** | .3428 | .2505 | .1609 |
| `DisAlign`-PSP | **.3018** | **.1593** | **.0924** | **.3121** | **.1990** | **.1194** | .3005 | .1644 | .0988 | **.3485** | **.2542** | **.1644** |

alignment are $O(NHt_2)$ and $O(H^2Nt_1)$, respectively, where $t_2$ is the inner-loop iteration number. Therefore, the total time complexity of proxy Stein path alignment is $O(NHt_2) + O(H^2Nt_1) = O(NHt_2 + H^2Nt_1)$. Since $H < N$, proxy Stein path alignment is much cheaper than Stein path alignment. Empirically, we set $H^* = [\frac{N}{2}]$.

### 2.4 Putting together

The total loss of `DisAlign` could be obtained by combining the losses of the rating prediction module and the embedding distribution alignment module. That is, the losses of `DisAlign` with Stein Path (`DisAlign`-**SP**) and Proxy Stein Path (`DisAlign`-**PSP**) are:

$$\min \mathcal{L}_{\texttt{DisAlign-SP}} = L_B + \lambda_{SP} L_{SP}, \ \min \mathcal{L}_{\texttt{DisAlign-PSP}} = L_B + \lambda_{PSP} L_{PSP}, \tag{9}$$

where $\lambda_{SP}$ and $\lambda_{PSP}$ are hyper-parameters to balance the two types of losses. In testing phase, one can predict the missing rating in the target domain by taking the inner product of user embeddings $\boldsymbol{U}$ and cold item embeddings $\boldsymbol{C}$.

## 3 Experiments

### 3.1 Experimental setup

**Datasets and Tasks.** We conduct extensive experiments on two popuarly used real-world datasets, i.e., *Douban* and *Amazon*. First, the **Douban** dataset [50, 51] has three domains, i.e., Book, Music, and Movie, which contains ratings, reviews, tags, and item details. There are six CDCSR tasks on Douban by randomly choosing two domains as source domain and target domain respectively. Second, the **Amazon** dataset [49, 27] has two domains, i.e., Movies and TV (Movie), and CDs and Vinyl (Music). There are two tasks on Amazon, i.e., Amazon Movie → Amazon Music and Amazon Music → Amazon Movie. For both datasets, we binarize the ratings to 1 and 0. Specifically, we take the ratings higher or equal to 4 as positive and others as negative. We also filter the users and items with less than 5 interactions, following existing research [46, 51]. We list the detailed information on these datasets and tasks in Section B.1 of the supplementary material.

**Baselines.** We compare our proposed `DisAlign` with the following state-of-the-art cold-start and CDR models. (1) **DropoutNet** [41] inputs both auxiliary representations and collaborative filtering representations and randomly dropouts pre-trained collaborative filtering representations for training.

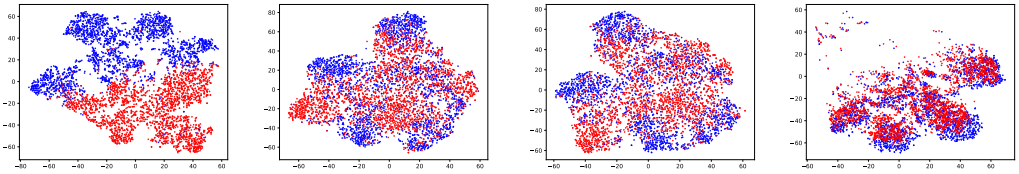

(a) Heater (b) ESAM (c) DARec (d) `DisAlign`-SP

Figure 5: The t-SNE visualization of **Douban Movie**→**Douban Book**, where **Douban Movie** is the source domain with red dots and **Douban Book** is the target domain with blue dots.

(2) **LLAE** [18] introduces semantic auto-encoder using the idea of zero-shot learning to solve the cold-start recommendation problem. (3) **Heater** [54] is the latest cold-start recommendation model which combines separate-training and joint-training framework to overcome the error superimposition issue. (4) **WCF** [26] is the first attempt to apply Wasserstein distance optimal transport for item cold-start recommendation. (5) **ESAM** [4] adopts attribute correlation alignment to improve long-tail recommendation performance by suppressing inconsistent distribution between displayed and non-displayed items. (6) **DARec** [46] adopts adversarial training strategy to extract and transfer knowledge patterns for shared users across domains and achieves the state-of-the-art performance in CDR. For **DropoutNet**, **LLAE**, **Heater**, and **WCF**, we use the same setting as reported in their original papers. For **DARec** and **ESAM**, since they cannot be directly applied to cold-start tasks, we adopt the same rating prediction module as `DisAlign`. Note that, for a fair comparison, all the models use the same types of data and pre-processing methods during experiments.

**Implemented details.** We provide the implemented details of our proposed model and baselines. The auxiliary representations for $\boldsymbol{X}^W$ and $\boldsymbol{X}^C$ across domains include genres, themes, reviews, item profiles, etc. We split auxiliary representations into each word and adopt directional skip-gram [33] on Douban for Chinese words and apply Glove [31] on Amazon for English words to obtain the average feature representations with dimension $Z = 200$. We use all the user-item rating interactions in the source domain, and all the items auxiliary representations in both the source domain and the target domain for training the model, following standard evaluation for unsupervised adaptation [22, 11]. For all the experiments, we perform five random experiments and report the average results. We choose Adam [16] as optimizer, and adopt Hit Rate@20 (HR@20), Recall@20, and NDCG@20 [43] as the ranking evaluation metrics.

**Hyper-parameter settings.** We set batch size $N = 256$ for both the source and target domains. The latent embedding dimension is set to $D = 128$. For the *rating prediction module*, we set the balance hyper-parameters as $\eta = 0.01$ and $\zeta = 0.01$, and number of cluster $K = 5$ for item unsupervised clustering. For the *stein path alignment module*, we set the moving step size as $\epsilon = 0.01$ and the kernel bandwidth as $\sigma = 0.5$. For the *proxy stein path alignment module*, we set $\alpha = 0.1$ and $H = 64$ according to Section 2.3.3. Finally, for the balance parameters, $\lambda_{SP}$ and $\lambda_{PSP}$ are first selected according to accuracy on **Douban Movie** → **Douban Book** and then fixed as the best values, i.e., $\lambda_{SP} = \lambda_{PSP} = 0.5$. Although there are many hyper-parameters, we first optimize the hyper-parameters of the rating prediction module, and then optimize the other hyper-parameters.

### 3.2 Recommendation performance

**Results and discussion.** The comparison results on Douban and Amazon datasets are shown in Table 1. From it, we can find that (1) Although **Heater** can get better results on conventional cold-start problem, it cannot achieve satisfying solutions on CDCSR problem since it cannot reduce the discrepancy across domains. (2) **WCF** obtains better performance than **Heater** in some tasks, but optimal transport with Wasserstein distance is easily affected by noisy samples, resulting in the over-adaptation errors in boundaries and limiting the transportation results. (3) **ESAM** and **DARec** provide correlated-attribution alignment and adversarial training to match source and target domains, while such coarsely matching methods lead to limited prediction enhancement. (4) `DisAlign`-**SP** or `DisAlign`-**PSP** consistently achieves the best performance, which proves that Stein path alignment strategy can significantly improve the prediction accuracy. (5) `DisAlign`-**PSP** outperforms `DisAlign`-**SP** on several tasks, e.g., Music and Movie domains on both datasets, which demostrates

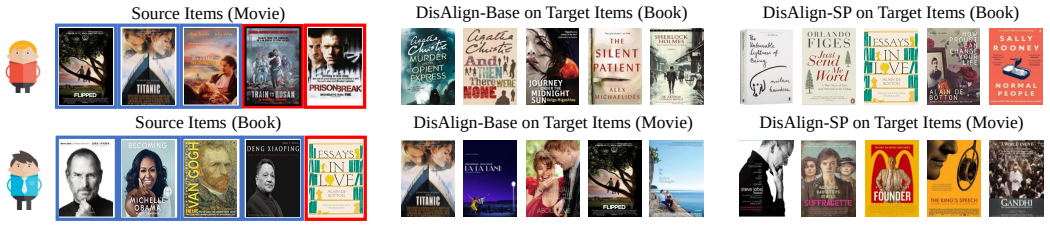


Figure 7: Case study on the recommendation task of **Douban Movie→Douban Book** and **Douban Book→Douban Movie**. The left part are the user preferences in the source domain. The middle and right parts are the recommendation results of `DisAlign`-Base and `DisAlign`-SP, respectively.

that typical proxies can filter out the outliers and improve model robustness. Besides, we further investigate the time consumption of each model on different tasks, and report the results in Figure 6. From it, we find that `DisAlign`**-SP** is the slowest, because it has to transport the whole batchsize of samples from the target domain to the source domain. In contrast, `DisAlign`**-PSP** is much faster than `DisAlign`**-SP**, and also faster than **WCF** and **DARec**, since it only needs to transport typical target proxies.

**Visualization.** To show the feature transferability, we visualize the t-SNE embeddings [17] of the source item auxiliary embeddings ($\boldsymbol{W}$) and the target item auxiliary embeddings ($\boldsymbol{C}$). The results of Douban Movie→Douban Book are shown in Figure 5. From it, we can see that (1) **Heater** does not has the ability to bridge the gap across different domains, and thus the embeddings are separated in source and target domains, as shown in Figure 5(a); (2) **ESAM** and **DARec** have the tendency to draw the source and target embeddings closer, while they still have a certain distance, as shown in Figure 5(b) and Figure 5(c). This indicates that they can only align the marginal probability distribution; (3) `DisAlign`**-SP** in Figure 5(d) depicts that the embeddings trained through Stein path alignment achieves more closer gap between the source and target domains. The visualization on Amazon dataset shows similar result, and we present it in Section B.2 of the supplementary material.

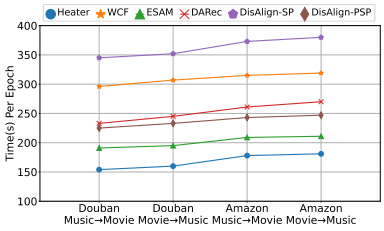


Figure 6: Comparison of running time on four tasks.

### 3.3 Analysis

**Ablation study.** To study how does each module of `DisAlign` contribute on the final performance, we compare `DisAlign` with its several variants, including `DisAlign`**-Base** and `DisAlign`**-SP(I)**. (1) `DisAlign`-Base only consists of the rating prediction module with collaborative embeddings clustering. (2) `DisAlign`-SP(I) only aligns the warm item auxiliary embedding $\boldsymbol{W}$ and the cold item auxiliary embedding $\boldsymbol{C}$. The comparison results are shown in Table 1. From it, we can observe that (1) `DisAlign`-Base without the Stein path distribution alignment module cannot transfer knowledge from the source domain to the target domain, resulting in poor performance, (2) `DisAlign`-SP(I) achieves better performance than `DisAlign`-Base, where we only align the distributions between $\boldsymbol{W}$ and $\boldsymbol{C}$, and (3) By extra aligning $\boldsymbol{C}$ with $\boldsymbol{V}$, `DisAlign`-SP can further promote the performance of `DisAlign`-SP(I). Overall, the above ablation study demonstrates that our proposed embedding distribution alignment module is effective in solving the CDCSR problem.

**Case study.** In order to illustrate the domain discrepancy problem mentioned in the Section 2.3 (Figure 3), we visualize the cases on **Douban Movie→Douban Book** and **Douban Book→Douban Movie**. Figure 7 shows the recommendation results. The left part is the user-item interactions in the source domain where the blue and red frames indicate users like or dislike the items respectively. The middle part denotes the top-5 recommendation results for the corresponding users based on `DisAlign`-Base, where we can see that these users will probably dislike the recommended items in the target domain due to the lack of embedding distribution alignment. After applying Stein path alignment on the right part, the recommender system can effectively improve the results. The results indirectly demonstrate that Stein path can properly translate the items across different domains according to the latent probability distribution.

**Parameter sensitivity.** We finally study the effects of hyper-parameters on model performance. First, we vary $\lambda_{SP}$ and $\lambda_{PSP}$ in $\{0.1, 0.3, 0.5, 0.7, 1, 3, 5, 10\}$ and report the results in Section B.3 of the supplementary materials. From it, we see that, the embedding distribution alignment module cannot play a central role in the training process when $\lambda_{SP}, \lambda_{PSP} \to 0$, bringing the discrepancy between the source and target domains. When $\lambda_{SP}$ and $\lambda_{PSP}$ become too large, the embedding distribution alignment module will suppress the rating prediction module, which also decreases the recommendation results. The above results indicate that choosing the proper hyper-parameters to balance the embedding distribution alignment loss and rating prediction loss can effectively improve the performance of `DisAlign`. Then, we study the effect of *embedding dimension* ($D$) on `DisAlign`, and report the results in Section B.4 of the supplementary materials. We find that the recommendation accuracy of `DisAlign`-SP and `DisAlign`-PSP increase with $D$, indicating that larger embedding can represent user and item preferences more precisely.

# 4 Related work

**Cold-start recommendation.** Existing approaches on this are mainly of two types, i.e., separate-training and joint-training. The former models, e.g., LinMap [9] and DeepMusic [40], separate the learning of the collaborative filtering embeddings and auxiliary embeddings, and thus always lead to error superimposition [54]. The later jointly minimizes the recommendation error on the user-item interaction and transformation function, including DropoutNet [41], LLAE [18], and Heater [54]. Among them, Heater [54] is the state-of-the-art model which integrates randomized training mechanism with mixture-of-experts to provide better performance. However, the above cold-start approaches cannot adjust to the CDCSR problem due to the discrepancy across different domains.

**Cross domain recommendation (CDR).** According to [52], existing CDR models have three main types, i.e., *transfer-based* methods, *clustered-based* methods, and *multitask-based* methods. Transfer-based methods [49, 25] learn a linear or nonlinear mapping function across domains. Some recent method [46] even adopts adversarial learning strategy to obtain more reliable knowledge across domains with shared users. Clustered-based methods [44] adopt co-clustering approach to learn cross-domain comprehensive embeddings by collectively leveraging single-domain and cross-domain information within a unified framework. Multi-task-based methods [15, 50, 51, 53] enable dual knowledge transfer across domains by introducing shared connection modules in neural networks. Nevertheless, conventional CDR approaches cannot solve the CSCDR problem where user-item interaction data in absent in the target domain.

**Domain adaptation.** Existing works on this are mainly of three types, i.e., *discrepancy-based* methods, *adversarial-based* methods, and *sample-based matching* methods [55, 36]. Discrepancy-based methods learn the domain-invariant embeddings by the adaptation layer for moment matching, e.g., Maximum Mean Discrepancy (MMD) [3], Correlation Alignment (CORAL) [34, 35], and Center Moment Discrepancy (CMD) [47]. Recently, ESAM [4] extends CORAL by utilizing attribution alignment for domain adaptation in long-tail item recommendation. Adversarial-based methods integrate a domain discriminator for adversarial training, e.g., Domain Adversarial Neural Network (DANN) [8] and Adversarial Discriminative Domain Adaptation (ADDA) [38]. Sample-based matching methods are mainly based on the optimal transport [6, 45], which have the ability of encoding class-structure in distributions for minimizing the global transportation cost. However, the above approaches cannot work well in CDCSR setting, because the latent representations are always more scattered, complicated, and diverse.

# 5 Conclusion

In this paper, we propose Distribution Alignment (`DisAlign`), which includes the *rating prediction module* and the *embedding distribution alignment module*, for solving the cross-domain cold-start recommendation problem. We innovatively propose Stein path alignment and proxy Stein path alignment for embedding alignment across domains. We also conducted extensive experiments to demonstrate the superior performance of our `DisAlign` model. In the future, we plan to extend `DisAlign` to multi-domain cold-start recommendation tasks and conduct more comprehensive experiments on new datasets. We will also modify our model to adapt to the situation where there are also user-item interactions in the target domain.

## 6 Acknowledgments

This work was supported in part by the National Key R&D Program of China (No.2018YFB1403001) and sponsored by CCF-AFSG Research Fund.

## References

[1] Liang Bai and Jiye Liang. Sparse subspace clustering with entropy-norm. In *International Conference on Machine Learning*, pages 561–568. PMLR, 2020.

[2] G. Baxter. Book review: Probability and related topics in physical sciences. *Bulletin of the American Mathematical Society*, 66(6):472–476, 1960.

[3] Karsten M Borgwardt, Arthur Gretton, Malte J Rasch, Hans-Peter Kriegel, Bernhard Schölkopf, and Alex J Smola. Integrating structured biological data by kernel maximum mean discrepancy. *Bioinformatics*, 22(14):e49–e57, 2006.

[4] Zhihong Chen, Rong Xiao, Chenliang Li, Gangfeng Ye, Haochuan Sun, and Hongbo Deng. Esam: Discriminative domain adaptation with non-displayed items to improve long-tail performance. In *SIGIR*, pages 579–588, 2020.

[5] Maurizio Ferrari Dacrema, Iván Cantador, Ignacio Fernández-Tobıas, Shlomo Berkovsky, and Paolo Cremonesi. Design and evaluation of cross-domain recommender systems.

[6] Bharath Bhushan Damodaran, Benjamin Kellenberger, Rémi Flamary, Devis Tuia, and Nicolas Courty. Deepjdot: Deep joint distribution optimal transport for unsupervised domain adaptation. In *Proceedings of the European Conference on Computer Vision (ECCV)*, pages 447–463, 2018.

[7] Pierre Del Moral. *Mean field simulation for Monte Carlo integration*. CRC press, 2013.

[8] Yaroslav Ganin, Evgeniya Ustinova, Hana Ajakan, Pascal Germain, Hugo Larochelle, François Laviolette, Mario Marchand, and Victor Lempitsky. Domain-adversarial training of neural networks. *The journal of machine learning research*, 17(1):2096–2030, 2016.

[9] Zeno Gantner, Lucas Drumond, Christoph Freudenthaler, Steffen Rendle, and Lars Schmidt-Thieme. Learning attribute-to-feature mappings for cold-start recommendations. In *2010 IEEE International Conference on Data Mining*, pages 176–185. IEEE, 2010.

[10] Jacob Goldberger, Geoffrey E Hinton, Sam Roweis, and Russ R Salakhutdinov. Neighbourhood components analysis. *Advances in neural information processing systems*, 17:513–520, 2004.

[11] Boqing Gong, Kristen Grauman, and Fei Sha. Connecting the dots with landmarks: Discriminatively learning domain-invariant features for unsupervised domain adaptation. In *International Conference on Machine Learning*, pages 222–230. PMLR, 2013.

[12] Jyotirmoy Gope and Sanjay Kumar Jain. A survey on solving cold start problem in recommender systems. In *2017 International Conference on Computing, Communication and Automation (ICCCA)*, pages 133–138. IEEE, 2017.

[13] Jun Han and Qiang Liu. Stein variational gradient descent without gradient. In *International Conference on Machine Learning*, pages 1900–1908. PMLR, 2018.

[14] Cheng-Kang Hsieh, Longqi Yang, Yin Cui, Tsung-Yi Lin, Serge Belongie, and Deborah Estrin. Collaborative metric learning. In *WWW*, pages 193–201, 2017.

[15] Guangneng Hu, Yu Zhang, and Qiang Yang. Conet: Collaborative cross networks for cross-domain recommendation. In *Proceedings of the 27th ACM international conference on information and knowledge management*, pages 667–676, 2018.

[16] D. Kingma and J. Ba. Adam: A method for stochastic optimization. *Computer Science*, 2014.

[17] Van Der Maaten Laurens and Geoffrey Hinton. Visualizing data using t-sne. *Journal of Machine Learning Research*, 9(2605):2579–2605, 2008.

[18] Jingjing Li, Mengmeng Jing, Ke Lu, Lei Zhu, Yang Yang, and Zi Huang. From zero-shot learning to cold-start recommendation. In *Proceedings of the AAAI Conference on Artificial Intelligence*, volume 33, pages 4189–4196, 2019.

[19] Pan Li and Alexander Tuzhilin. Ddtcdr: Deep dual transfer cross domain recommendation. In *WSDM*, pages 331–339, 2020.

[20] Qiang Liu. Stein variational gradient descent as gradient flow. *arXiv preprint arXiv:1704.07520*, 2017.

[21] Qiang Liu and Dilin Wang. Stein variational gradient descent: A general purpose bayesian inference algorithm. *arXiv preprint arXiv:1608.04471*, 2016.

[22] Mingsheng Long, Yue Cao, Jianmin Wang, and Michael Jordan. Learning transferable features with deep adaptation networks. In *International conference on machine learning*, pages 97–105. PMLR, 2015.

[23] Mingsheng Long, Zhangjie Cao, Jianmin Wang, and Michael I Jordan. Conditional adversarial domain adaptation. In *Advances in Neural Information Processing Systems*, pages 1647–1657, 2018.

[24] Qianli Ma, Jiawei Zheng, Sen Li, and Gary W Cottrell. Learning representations for time series clustering. *Advances in neural information processing systems*, 32:3781–3791, 2019.

[25] Tong Man, Huawei Shen, Xiaolong Jin, and Xueqi Cheng. Cross-domain recommendation: An embedding and mapping approach. In *IJCAI*, pages 2464–2470, 2017.

[26] Yitong Meng, Xiao Yan, Weiwen Liu, Huanhuan Wu, and James Cheng. Wasserstein collaborative filtering for item cold-start recommendation. In *Proceedings of the 28th ACM Conference on User Modeling, Adaptation and Personalization*, pages 318–322, 2020.

[27] Jianmo Ni, Jiacheng Li, and Julian McAuley. Justifying recommendations using distantly-labeled reviews and fine-grained aspects. In *EMNLP-IJCNLP*, pages 188–197, 2019.

[28] Feiping Nie, Xiaoqian Wang, and Heng Huang. Clustering and projected clustering with adaptive neighbors. In *Proceedings of the 20th ACM SIGKDD International Conference on Knowledge Discovery and Data Mining*, KDD '14, page 977–986, 2014.

[29] Travis A O'Brien, William D Collins, Sara A Rauscher, and Todd D Ringler. Reducing the computational cost of the ecf using a nufft: A fast and objective probability density estimation method. *Computational Statistics & Data Analysis*, 79:222–234, 2014.

[30] Travis A O'Brien, Karthik Kashinath, Nicholas R Cavanaugh, William D Collins, and John P O'Brien. A fast and objective multidimensional kernel density estimation method: fastkde. *Computational Statistics & Data Analysis*, 101:148–160, 2016.

[31] Jeffrey Pennington, Richard Socher, and Christopher Manning. Glove: Global vectors for word representation. volume 14, pages 1532–1543, 01 2014.

[32] Steffen Rendle, Christoph Freudenthaler, Zeno Gantner, and Lars Schmidt-Thieme. Bpr: Bayesian personalized ranking from implicit feedback. *arXiv preprint arXiv:1205.2618*, 2012.

[33] Yan Song, Shuming Shi, Jing Li, and Haisong Zhang. Directional skip-gram: Explicitly distinguishing left and right context for word embeddings. In *Proceedings of the 2018 Conference of the North American Chapter of the Association for Computational Linguistics: Human Language Technologies, Volume 2 (Short Papers)*, pages 175–180, 2018.

[34] Baochen Sun and Kate Saenko. Deep coral: Correlation alignment for deep domain adaptation. In *European conference on computer vision*, pages 443–450. Springer, 2016.

[35] B. Sun and K. Saenko. Deep coral: Correlation alignment for deep domain adaptation. *Springer International Publishing*, 2016.

[36] Chuanqi Tan, Fuchun Sun, Tao Kong, Wenchang Zhang, Chao Yang, and Chunfang Liu. A survey on deep transfer learning. In *International conference on artificial neural networks*, pages 270–279. Springer, 2018.

[37] Eric Tzeng, Judy Hoffman, Trevor Darrell, and Kate Saenko. Simultaneous deep transfer across domains and tasks. In *Proceedings of the IEEE international conference on computer vision*, pages 4068–4076, 2015.

[38] Eric Tzeng, Judy Hoffman, Kate Saenko, and Trevor Darrell. Adversarial discriminative domain adaptation. In *CVPR*, pages 7167–7176, 2017.

[39] Evgeniya Ustinova and Victor Lempitsky. Learning deep embeddings with histogram loss. *arXiv preprint arXiv:1611.00822*, 2016.

[40] Aäron Van Den Oord, Sander Dieleman, and Benjamin Schrauwen. Deep content-based music recommendation. In *NIPS*, volume 26. Neural Information Processing Systems Foundation (NIPS), 2013.

[41] Maksims Volkovs, Guang Wei Yu, and Tomi Poutanen. Dropoutnet: Addressing cold start in recommender systems. In *NIPS*, pages 4957–4966, 2017.

[42] D. Wang, Z. Tang, C. Bajaj, and Q. Liu. Stein variational gradient descent with matrix-valued kernels. *Advances in neural information processing systems*, 32:7834–7844, 2019.

[43] Xiang Wang, Xiangnan He, Yixin Cao, Meng Liu, and Tat-Seng Chua. Kgat: Knowledge graph attention network for recommendation. In *Proceedings of the 25th ACM SIGKDD International Conference on Knowledge Discovery & Data Mining*, pages 950–958, 2019.

[44] Yaqing Wang, Chunyan Feng, Caili Guo, Yunfei Chu, and Jenq-Neng Hwang. Solving the sparsity problem in recommendations via cross-domain item embedding based on co-clustering. In *Proceedings of the Twelfth ACM International Conference on Web Search and Data Mining*, pages 717–725, 2019.

[45] Renjun Xu, Pelen Liu, Liyan Wang, Chao Chen, and Jindong Wang. Reliable weighted optimal transport for unsupervised domain adaptation. In *CVPR*, pages 4394–4403, 2020.

[46] Feng Yuan, Lina Yao, and Boualem Benatallah. Darec: Deep domain adaptation for cross-domain recommendation via transferring rating patterns. *arXiv preprint arXiv:1905.10760*, 2019.

[47] Werner Zellinger, Thomas Grubinger, Edwin Lughofer, Thomas Natschläger, and Susanne Saminger-Platz. Central moment discrepancy (cmd) for domain-invariant representation learning. *arXiv preprint arXiv:1702.08811*, 2017.

[48] Hongyuan Zha, Xiaofeng He, Chris Ding, Ming Gu, and Horst D Simon. Spectral relaxation for k-means clustering. In *NIPS*, pages 1057–1064, 2001.

[49] Cheng Zhao, Chenliang Li, Rong Xiao, Hongbo Deng, and Aixin Sun. Catn: Cross-domain recommendation for cold-start users via aspect transfer network. pages 229–238, 07 2020.

[50] Feng Zhu, Chaochao Chen, Yan Wang, Guanfeng Liu, and Xiaolin Zheng. Dtcdr: A framework for dual-target cross-domain recommendation. In *CIKM*, pages 1533–1542, 2019.

[51] Feng Zhu, Yan Wang, Chaochao Chen, Guanfeng Liu, and Xiaolin Zheng. A graphical and attentional framework for dual-target cross-domain recommendation. In *IJCAI*, pages 3001–3008, 2020.

[52] Feng Zhu, Yan Wang, Chaochao Chen, Jun Zhou, Longfei Li, and Guanfeng Liu. Cross-domain recommendation: Challenges, progress, and prospects. In *IJCAI*, pages 4721–4728. ijcai.org, 2021.

[53] Feng Zhu, Yan Wang, Jun Zhou, Chaochao Chen, Longfei Li, and Guanfeng Liu. A unified framework for cross-domain and cross-system recommendations. *IEEE Transactions on Knowledge and Data Engineering*, 2021.

[54] Ziwei Zhu, Shahin Sefati, Parsa Saadatpanah, and James Caverlee. Recommendation for new users and new items via randomized training and mixture-of-experts transformation. In *SIGIR*, pages 1121–1130, 2020.

[55] Fuzhen Zhuang, Zhiyuan Qi, Keyu Duan, Dongbo Xi, Yongchun Zhu, Hengshu Zhu, Hui Xiong, and Qing He. A comprehensive survey on transfer learning. *Proceedings of the IEEE*, 109(1):43–76, 2021.